

**Simulation of current-filament dynamics and relaxation in the Pegasus
Spherical Tokamak.**

(10 August 2012)

J.B. O'Bryan, C.R. Sovinec, and T.M. Bird

*Department of Engineering Physics, University of Wisconsin, 1500 Engineering Drive,
Madison, Wisconsin 53706 USA*

Copyright 2012 American Institute of Physics. This article may be downloaded for personal use only. Any other use requires prior permission of the author and the American Institute of Physics. The following article appeared in [J.B. O'Bryan, C.R. Sovinec, and T.M. Bird. Phys. Plas. 19, 080701 \(2012\)](#) and may be found at <http://link.aip.org/link/?PHP/19/080701>.

NOTICE:

This report was prepared as an account of work sponsored by the United States Government. Neither the United States nor the United States Department of Energy, nor any of their employees, nor any of their contractors, subcontractors, or their employees, makes any warranty, expressed or implied, or assumes any legal liability or responsibility for the accuracy, completeness, or usefulness of any information, apparatus, product or process disclosed or represents that its use would not infringe privately owned rights.

Simulation of current-filament dynamics and relaxation in the Pegasus Spherical Tokamak.

J.B. O'Bryan,^{1, a)} C.R. Sovinec,¹ and T.M. Bird¹

*Department of Engineering Physics, University of Wisconsin, Madison,
Wisconsin 53706*

(Dated: 10 August 2012)

Nonlinear numerical computation is used to investigate the relaxation of non-axisymmetric current-channels from washer-gun plasma sources into “tokamak-like” plasmas in the Pegasus Toroidal Experiment [N.W. Eidietis *et al.* *J. Fus. En.* (2007)]. Resistive MHD simulations with the NIMROD code [C.R. Sovinec *et al.* *Phys. Plas.* 2003] utilize ohmic heating, temperature-dependent resistivity, and anisotropic, temperature-dependent thermal conduction corrected for regions of low magnetization to reproduce critical transport effects. Adjacent passes of the simulated current-channel attract and generate strong reversed current sheets that suggest magnetic reconnection. With sufficient injected current, adjacent passes merge periodically, releasing axisymmetric current rings from the driven channel. The current rings have not been previously observed in helicity injection for spherical tokamaks, and as such, provide a new phenomenological understanding for filament relaxation in Pegasus. After large-scale poloidal-field reversal, a hollow current profile and significant poloidal flux amplification accumulate over many reconnection cycles.

PACS numbers: 52.55.Fa, 52.30.Cv, 52.25.Fi, 02.60.-x

^{a)}Electronic mail: jobryan@wisc.edu

Geometric constraints on the central solenoids of spherical tokamaks limit the capacity for current drive through ohmic induction, and non-inductive current drive can be used to expand their operational regimes. DC helicity injection through localized washer-gun plasma sources is being investigated as a means of non-inductive startup on the Pegasus Toroidal Experiment (University of Wisconsin).¹ The 1 cm diameter bore plasma guns emit plasma when a gas feed is arced over alternating conducting and insulating washers within each gun.² A separate DC bias drives current through emitted plasma along the magnetic field lines that connect the plasma gun(s) (cathode) and the stainless steel anode. The development and relaxation of current filaments produces startup current in Pegasus. This paper reports on nonlinear MHD modeling of this process in configurations where the plasma guns are mounted in the lower divertor region. Our simulation results support a unique phenomenology of relaxation as an accumulation of axisymmetric current rings that are released when current-channel passes merge and reconnect.

In divertor gun discharges, the vacuum vessel is initially filled with neutral gas with a pre-fill pressure of $1 - 5 \times 10^{-5}$ Torr.³ Prior to the application of a bias voltage to drive current, plasma is emitted from the guns, transporting particles and heat into the background. During helicity injection, Ohmic heating occurs along the current filament path.

Initially, the current-channels wind along the helical vacuum magnetic field lines. When the self-induced magnetic field from DC current is large enough to change the sign of poloidal flux at the center column, $I_p \approx 15$ kA, the helical gun plasma relaxes toward a “tokamak-like” configuration.^{3,4} Here, a “tokamak-like” plasma is defined such that the toroidally averaged magnetic fields indicate nested poloidal flux surfaces with a diffuse current profile. Unlike spheromaks and spherical tokamaks driven by coaxial helicity injection,^{5,6} where an initially axisymmetric plasma transitions to a non-axisymmetric state after crossing some stability boundary, the initial plasma state in Pegasus is three-dimensional and relaxes toward an axisymmetric tokamak equilibrium state.

Magnetic diagnostics indicate the presence of $n = 1$ MHD activity during helicity injection with the plasma guns, typically in the 10 – 20 kHz frequency range.³ This MHD activity is not observed during ohmic startup, nor is the MHD activity observed after cessation of DC helicity injection. The presence of MHD activity only during helicity injection and formation of a tokamak-like state suggests it is an important part of the relaxation process. Equilibrium reconstruction using experimental flux-loop measurements produces hollow current profiles for the relaxed state, and the current density peaks at the normalized poloidal flux value of $\psi_N \approx 0.7$.³ This result suggests that the plasma guns serve as sources of edge current drive that must diffuse classically or otherwise into the plasma core.

While the initial helical plasma state and final relaxed plasma state are well diagnosed in the experiment, the dynamics of the relaxation process have not been directly observed. Diagnostics that provide multidimensional information, such as the soft x-ray camera, are unable to temporally resolve the interactions between the helical filaments. The magnetic diagnostics resolve fluctuations temporally, but are incapable of spatially resolving the fine-scale structure of the current filaments.

Here, we apply numerical computation to investigate details of the relaxation process which have not been directly observed in the experiment. The temporal evolution of a three-dimensional current filament is modeled with the NIMROD code⁷, starting from vacuum fields and progressing through relaxation into a tokamak-like state. The computations presented in this paper use a single-temperature, resistive MHD model. Temperature-dependent anisotropic thermal conduction, temperature-dependent resistivity, and ohmic heating re-

produce critical transport effects as the warm filament evolves in cooler background plasma. A similar model has been applied successfully to understand the interaction between thermal transport and magnetic relaxation in the SSPX spheromak.⁸⁻¹⁰

The initial condition of our Pegasus simulations is treated as plasma with respect to transport properties, albeit at an unphysically low temperature of 0.25 eV ($x_i \equiv \omega_{ci}\tau_i \approx 0.025$, where τ_i is the ion collision time). The initial electron number density is set to $1 \times 10^{19} \text{ m}^{-3}$, and ionization energy is not considered in our modeling. However, transitions from unmagnetized transport properties to magnetized properties over the profile are important. We therefore use the Braginskii formulation¹¹ for ion κ_{\perp} ,

$$\kappa_{\parallel} \approx \kappa_{\parallel e} = \frac{n_e T_e \tau_e \gamma_{0e}}{m_e \delta_{0e}} \quad (1)$$

$$\kappa_{\perp} \approx \kappa_{\perp i} = \frac{n_i T_i \tau_i}{m_i} \frac{\gamma_{1i} x_i^2 + \gamma_{0i}}{x_i^4 + \delta_{1i} x_i^2 + \delta_{0i}} \quad , \quad (2)$$

which reproduces the transition from unmagnetized ($x_i \ll 1$) to magnetized ($x_i \gg 1$) thermal conduction as the local plasma temperature increases. Our results show significant 3D spatial variation in the magnetization parameter x_i , with $x_i \gg 1$ near the driven current-channel and $x_i \ll 1$ near the domain boundary.

Current injection from the washer guns is modeled with a spatially localized ad-hoc force density on the electrons that acts as a source in the combined Faraday / Ohm's Law within a very small fraction of the domain. The effective applied electric field, \mathbf{E}_{inj} in Ohm's law, $\mathbf{E} + \mathbf{v} \times \mathbf{B} = \eta \mathbf{J} - \mathbf{E}_{inj}$, sustains current density in the presence of resistive dissipation. The poloidal localization of the source (Figure 1) is aligned with the vacuum magnetic field pitch angle. The effective applied electric field is parallel to the total magnetic field, i.e. $\mathbf{E}_{inj} = \lambda_{inj}(\mathbf{x}, t) \mathbf{B}$, where λ_{inj} is the drive parameter, including spatial localization. The magnitude of the applied electric field increases linearly in time.

The application of the localized force density directly induces a helical magnetic field perturbation, which initially produces current density just in the vicinity of the source. The magnetic forces at the ends of the perturbation launch torsional Alfvén waves that carry current density along the vacuum magnetic field on an Alfvénic time-scale. Over a longer time-scale, perpendicular, resistive diffusion of the magnetic perturbation results in net current.

At low injected current, the current in the computations streams along the helical vacuum magnetic field lines (Figure 1), as observed during experimental discharges. After the self-induced magnetic field locally exceeds the vacuum magnetic field around the current-channel, the channel begins to oscillate in the poloidal plane from the attractive Lorentz force between adjacent passes. When the displacement of adjacent passes is sufficiently large, conditions of relatively good electrical conductivity exist between the two colliding passes. At locations of such merging, the presence of a strong reversed current sheet between the two adjacent passes of the current-channel (Figure 2a) indicates magnetic reconnection. A two-dimensional cross-section of the initial current pass attraction appears to be similar to Sweet-Parker reconnection from a study of parallel merging co-helicity flux tubes,^{12,13} but the magnetic reconnection between adjacent passes of current filaments in Pegasus is fundamentally three-dimensional in nature.

After the self-induced magnetic field of the current-channel further exceeds the vacuum magnetic field, adjacent passes of the current-channel fully reconnect. Unlike results for

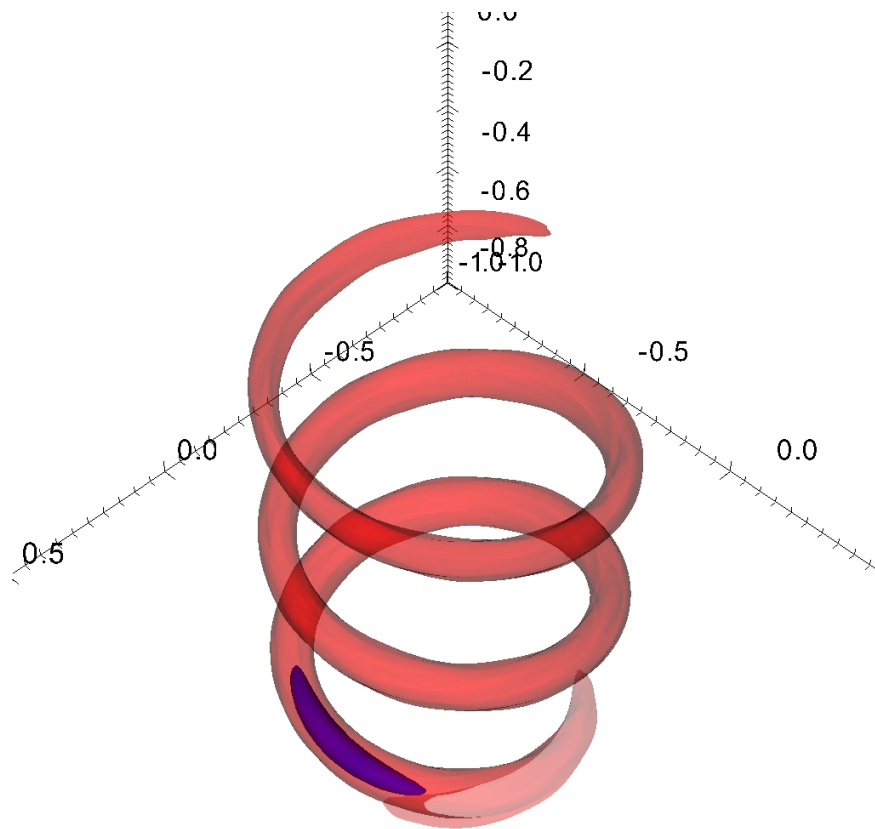


FIG. 1. The spatial distribution of λ_{inj} (half-max shown in blue) and the resulting helically winding current-channel ($\lambda = 1.0 \text{ m}^{-1}$ shown in translucent red) are shown at $I_p \approx 0.85 \text{ kA}$.

parallel co-helicity flux tubes,¹⁴ the current-channel passes in our simulations do not remain merged, but separate with a changed connectivity that severs an axisymmetric current loop (Figure 3) from a shortened driven current-channel. The dynamics of this process are visualized with the animation of λ -isosurfaces shown in Fig. 3. An oblique contact angle between adjacent passes does not explain the eventual separation, as coalescence is predicted over a significant range of contact angle for co-helicity flux tubes.¹⁴ Note that unlike the configuration in Ref. 14, after reconnection, only the helical path contains drive, while the symmetric ring freely decays. The separated current rings are formed slightly inboard of the current-channel near the midplane and slowly propagate vertically away from the gun. After large-scale field reversal, current rings that remain coherent stagnate at the top of the region where poloidal flux is amplified relative to the initial state (Figure 4).

Relatively higher pressure in the inflow region than in the compressed outflow region creates an elongated x-type structure. An elongated current sheet is observed in computations after the passes stagnate in the inflow direction and slide past one another in the outflow direction (Figure 2b) during current ring formation. The loss of drive causes the upper pass to move radially inward as it separates from the current-channel. Magnetic pressure from the self-induced field correspondingly causes the driven lower pass to move radially outward.

Current ring formation occurs rapidly, with a time-scale of approximately $50 \mu\text{s}$ from when adjacent passes first make contact to the release of the current ring, relative to the

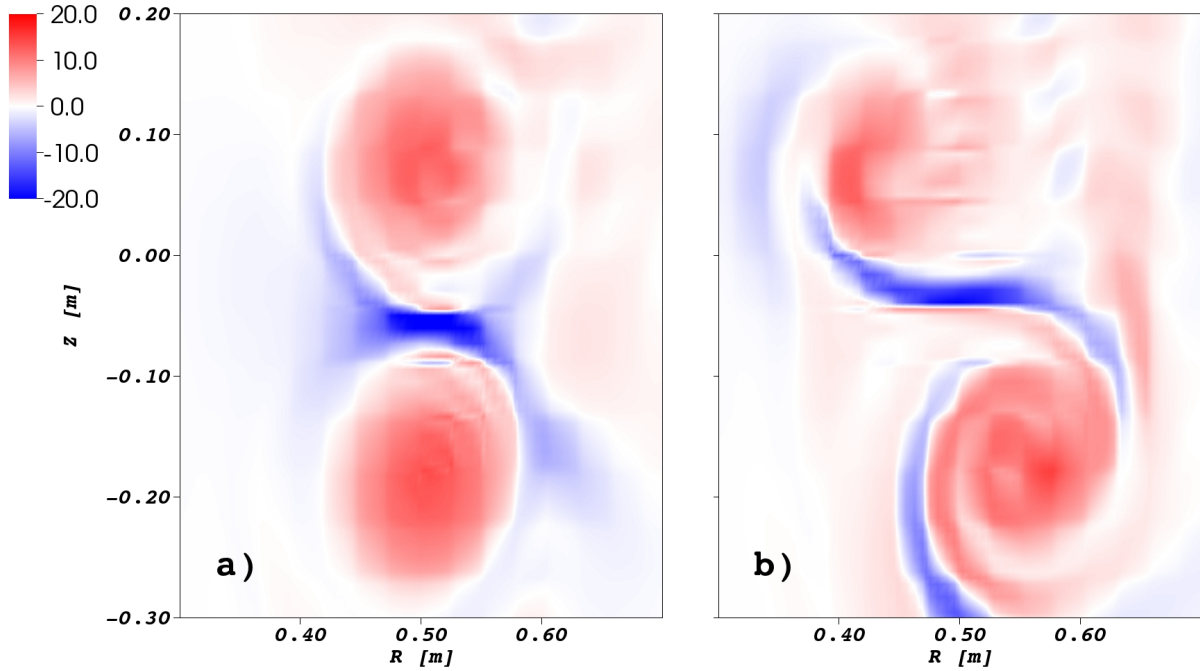


FIG. 2. Magnetic reconnection is indicated by the presence of strong reverse currents when adjacent passes of the current-channel come into contact. Contours of $\lambda = \mu_0 J_{\parallel} / B$ in units of m^{-1} are shown at $\phi = 0$ (a) at the instance of closest approach and (b) as the channel passes “slide” past one another.

typical stagnation and relatively slow merger of 2D flux tubes. When the current loops are first observed, $I_p \approx 4$ kA, current rings form on an average interval of approximately $250 \mu\text{s}$. The length of the interval gradually increases to $800 - 900 \mu\text{s}$ for $I_p > 40$ kA. Most of the current within a ring filament diffuses within approximately $100 \mu\text{s}$ of its release from the driven current channel.

The current from our simulated axisymmetric rings redistributes along the edge of the amplified-flux region, forming a hollow current profile (Figure 4). Shortly after large-scale magnetic field reversal, current flows diffusely along the inboard side of the amplified-flux region. At larger I_p , current on the inboard side flows in a distinct channel that connects to the outboard driven current-channel. After large-scale magnetic field reversal, significant poloidal flux amplification is observed (1.5 mWb at $I_p \approx 36$ kA), having accumulated over many reconnection cycles.

Prior to large-scale poloidal-field reversal, most of the heat is transported to the electrodes, Figure 5 (a)&(b). After large-scale poloidal-field reversal, a significant fraction of thermal energy recirculates in the amplified-flux region, Figure 5 (c)&(d). The formation of axisymmetric current rings produces significant heat flux, as shown by the parallel heat flux contours. The large thermal transport creates a more diffuse plasma temperature profile in the plasma core. The large current density in the reconnection current sheet and current rings also results in significant ohmic heating of the plasma outside the current-channel. In the vicinity of the reconnection, the convective heat flux (not shown) transiently exceeds the parallel conductive heat flux.

The 3D reconnection between adjacent current passes is similar to reconnection observed

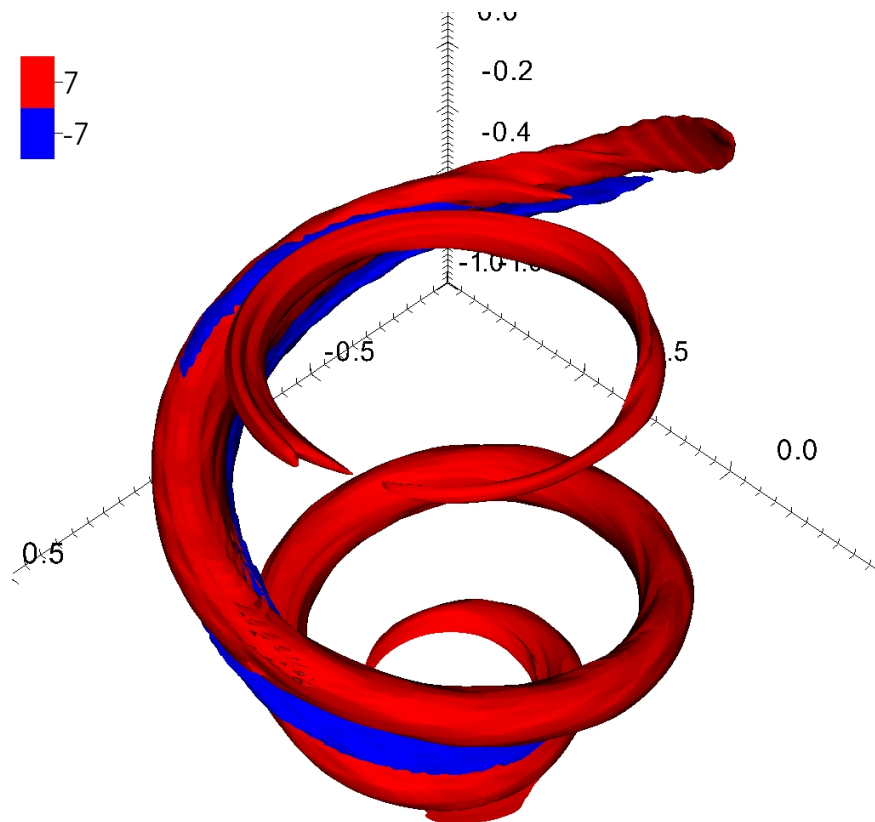


FIG. 3. Reconnection releases a current ring (shown in the center of the figure) from the driven channel plasma. Isosurfaces of $\lambda = \pm 7 \text{ m}^{-1}$ are shown. (enhanced online) [URL: <http://dx.doi.org/10.1063/1.4746089.1>].

in the Reconnection Scaling eXperiment (RSX).^{15,16} In RSX, two plasma guns produce initially parallel current filaments, which undergo a kink instability that causes the current filaments to helically gyrate. Cross-sections of measured magnetic field and current density resemble typical flux tube merger theory.¹⁶ Impulsive reconnection between the filaments produces patchy regions of 3D reconnection, which is analogous to the reconnection during current ring formation in our simulations.

The axisymmetric current rings released from the filaments in our simulations have not been previously observed for helicity injection in spherical tokamaks, and as such, provide a new phenomenological understanding for filament relaxation in Pegasus. The current rings provide the mechanism for poloidal flux amplification over multiple reconnection events. The thermal energy released from the current rings into the plasma core may contribute to the centrally peaked pressure profile observed in equilibrium reconstructions of relaxed plasmas in the experiment. The hollow current profile produced in our simulations is also consistent with the current profiles in the equilibrium reconstructions.

We acknowledge that two-fluid effects may significantly influence current-channel interaction. The experimentally measured electron density $n_e \approx 5 \times 10^{18} \text{ m}^{-3}$ during a typical non-solenoidal discharge¹⁷ produces a Hall parameter of $\delta_i/r_c \approx 3.6$ for a current-channel width $r_c = 4 \text{ cm}$, where δ_i is the ion skin depth. A large Hall parameter indicates that

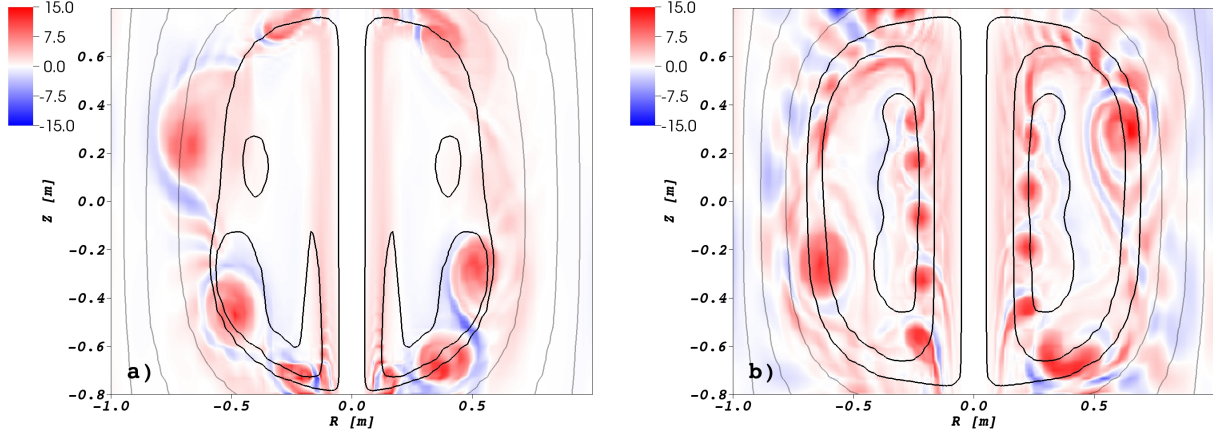


FIG. 4. A hollow current profile is observed after large-scale magnetic field reversal during helicity injection. (a) Diffuse inboard current is observed at $I_p \approx 26$ kA. (b) A distinct inboard channel is observed at $I_p \approx 42$ kA. Contours of λ in units of m^{-1} are shown. The overlaid contour lines show the poloidal flux function, where the darker contours correspond to the amplified-flux region.

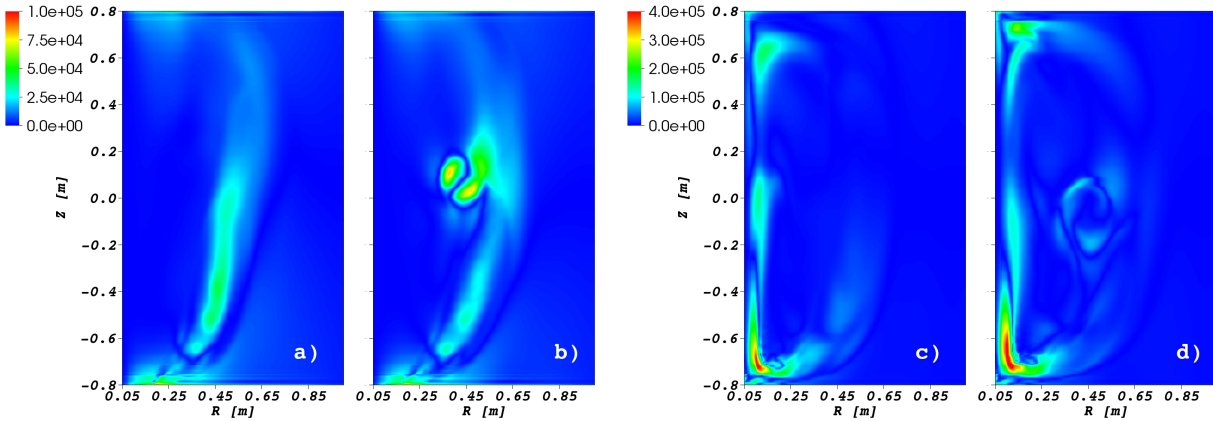


FIG. 5. Magnitude of toroidally-averaged parallel heat flux, $\left| \frac{1}{2\pi} \int_{-\pi}^{\pi} n \chi_{\parallel} \mathbf{b} \mathbf{b} \cdot \nabla T d\phi \right|$, in units of W/m^2 where χ_{\parallel} is the parallel thermal diffusivity. Figures (a)&(b) (plotted to same scale) show parallel heat flux prior to large-scale poloidal field reversal, $I_p \approx 6.5$ kA, where (a) corresponds to a period between current ring formation and (b) corresponds to when a current ring is present. Figures (c)&(d) (plotted to same scale) show parallel heat flux after large-scale poloidal field reversal, $I_p \approx 20$ kA, where (c) corresponds to a period between current ring formation and (d) corresponds to when a current ring is present.

the electron fluid can decouple from the ion fluid, affecting current-channel motion and interaction. Two-dimensional flux tube merger results with an extended-MHD Ohm's Law predicts a larger current sheet thickness with a more gradual drop-off than predicted by MHD theory.^{12,13} Our future simulation work on current-channel evolution in Pegasus will address two-fluid effects.

We would like to acknowledge valuable discussions with Professor Ray Fonck, Dr. Aaron Redd, and other members of the Pegasus team. This work is supported by the U.S. Depart-

ment of Energy grant DE-FC02-05ER54813 as part of the Plasma Science and Innovation Center. Computations have been performed at the National Energy Research Scientific Computing Center, which is supported by the Office of Science of the U.S. Dept. of Energy under Contract No. DE-AC02-05CH11231.

REFERENCES

- ¹D.J. Battaglia, M.W. Bongard, R.J. Fonck, and A.J. Redd, *Nucl. Fus.* **51**, 073029 (2011).
- ²A.J. Redd, D.J. Battaglia, M.W. Bongard, R.J. Fonck, E.T. Hinson, B.A. Kujak-Ford, B.T. Lewicki, A.C. Sontag, and G.R. Winz, *J. Fus. En.* **28**, 203 (2009).
- ³N.W. Eidietis, Ph.D. thesis, University of Wisconsin–Madison, 2007.
- ⁴N.W. Eidietis, R.J. Fonck, G.D. Garstka, E.A. Unterberg, and G.R. Winz, *J. Fus. En.* **26**, 43 (2007).
- ⁵R. Raman, T.R. Jarboe, W.T. Hamp, A.J. Redd, B.A. Nelson, R.G. O’Neill, P.E. Sieck, and R.J. Smith, *Phys. Plas.* **14**(2), 022504 (2007).
- ⁶S. Woodruff, D.N. Hill, B.W. Stallard, R. Bulmer, B. Cohen, C.T. Holcomb, E.B. Hooper, H.S. McLean, J. Moller, and R.D. Wood, *Phys. Rev. Lett.* **90**(9), 095001 (2003).
- ⁷C.R. Sovinec, T.A. Gianakon, E.D. Held, S.E. Kruger, D.D. Schnack, and the NIMROD Team, *Phys. Plas.* **10**(5), 1727–1732 (2003).
- ⁸C.R. Sovinec, B.I. Cohen, G.A. Cone, E.B. Hooper, and H.S. McLean, *Phys. Rev. Lett.* **94**(3), 035003 (2005)
- ⁹B.I. Cohen, E.B. Hopper, R.H. Cohen, D.N. Hill, H.S. McLean, R.D. Wood, S. Woodruff, C.R. Sovinec, and G.A. Cone, *Phys. Plas.* **12**(5), 056106 (2005).
- ¹⁰E.B. Hooper, B.I. Cohen, H.S. McLean, R.D. Wood, C.A. Ramero-Talamás, and C.R. Sovinec, *Phys. Plas.* **15**(3), 032502 (2008).
- ¹¹S.I. Braginskii, *Rev. Plas. Phys.* **1**, 205–311 (1965).
- ¹²J.A. Breslau, Ph.D. thesis, Princeton University, 2001.
- ¹³J.A. Breslau and S.C. Jardin, *Phys. Plas.* **10**(5), 1291–1298 (2003).
- ¹⁴M.G. Linton, R.B. Dahlburg, and S.K. Antiochos, *Astrophys. J.* **553**, 905–92 (2001).
- ¹⁵I. Furno, T.P. Intrator, E.W. Hemsing, S.C. Hsu, S. Abbate, P. Ricci, and G. Lapenta, *Phys. Plas.* **12**, 055702 (2005).
- ¹⁶T.P. Intrator, X. Sun, G. Lapenta, L. Dorf, and I. Furno, *Nat. Phys* **5**(7):521–526 (2009).
- ¹⁷D.J. Battaglia, M.W. Bongard, R.J. Fonck, A.J. Redd, and A.C. Sontag, *Phys. Rev. Lett.* **102**, 225003 (2009).